Using DPS Measurements for PTA with System Identification

Ammiwala, Huzefa

Publication date
2019

Citation (APA)
Ammiwala, H. (2019). *Using DPS Measurements for PTA with System Identification*.

INTEGRATED SYSTEMS APPPROACH FOR PETROLEUM PRODUCTION

ISAPP Project: Coupled Well-Reservoir Models for Pressure Transient Analysis in Horizontal Wells

Report

Using DPS Measurements for PTA with System Identification

February 2019

Delft University of Technology (TU Delft), The Netherlands
Faculty of Civil Engineering and Geosciences
Department of Geoscience and Engineering

Author:
Ir. M.H. Ammiwala (TU Delft),
m.h.ammiwala@tudelft.nl
(Post graduate researcher)

Supervisors:
Prof. dr. ir. Jan Dirk Jansen (TU Delft)
j.d.jansen@tudelft.nl

Dr. Aris Twerda (TNO)
aris.twerda@tno.nl

Dr. D.V. Voskov (TU Delft)
d.v.voskov@tudelft.nl

Abstract

Pressure measurements obtained with distributed pressure sensing (DPS) could be used to estimate circumferentially averaged reservoir parameters with pressure transient analysis (PTA). System identification (SI) for PTA allows us to estimate parameters such as permeability with dynamic bottom hole pressure and flow rates measurements, with the benefit of not having to rely on constant flow rates as input signals as required in traditional well testing. The focus of this research is: (1) flow rate estimation based on DPS data for vertical and deviated wells, (2) introducing a workflow for parameter estimation with SI for PTA with DPS measurements and (3) applying the workflow to numerical simulations of a well test to investigate the scope for using SI as a PTA method. With the friction component of the pressure drop between two sensors, the flow rates over the reservoir section can be estimated. Subsequently, the estimated flow rates and the pressure measurements during well operation are used to estimate a transfer function based on the data and are compared to analytical transfer functions in the frequency domain. Numerical experiments with a simulated vertical well showed that the flow rate can be estimated, and the permeability profile along the well bore can be constructed for homogenous, layered and heterogeneous reservoirs. Numerical experiments with a simulated deviated well showed that measurements errors have most effect at the bottom of the well.

1 Introduction

'Distributed' pressure sensors (DPS) in horizontal or deviated wells (i.e. arrays of pressure sensors with a relatively small spacing compared to the length of the completed zone) can be used to estimate the inflow from the reservoir and/or the flow rate in the wellbore [1]. The combination of estimated flow rates and measured pressures in the well bore offers opportunities to develop new methods for well testing. In particular, it may be possible to infer local differences in (circumferentially averaged) near-well permeabilities or skin values along the well. A new approach was developed to perform pressure transient analysis (PTA) based on the use of System Identification (SI) methods as used in the process industry [2].

Testing of a new PTA procedure should eventually be done with field data. However, as a first step, the use of synthetic data will be necessary to test the concept, assess the potential scope, and design an experimental setup. Synthetic data is generated with a coupled well bore and reservoir simulator with an accurate description of the well. One of the benefits of using SI for well testing is that it can handle arbitrary flow rates as input [2], which led to the development of a variable choke size as an alternative well control [3]. The use of SI for PTA was tested with a horizontal well model for reservoir parameter estimation [4]. Limitations of that research were neglect of errors, the use of a homogeneous reservoir model and the absence of using a deviated well as a test case.

The goal of this report is to assess the potential of DPS and to generate synthetic well testing results to identify reservoir properties with PTA by SI. To reach this objective the first step is to briefly review the previous work relating DPS, PTA, and SI. This is followed by a workflow that describes the steps from initialization of a coupled reservoir – well bore model to the identification of reservoir properties with SI. Two types of numerical experiments with synthetic data are conducted to validate the application of DPS for PTA with SI, the first with a vertical well, the second experiment with a deviated well.

2 Background

A brief overview of (well-known) concepts, distributed pressure sensing (DPS), pressure transient analysis (PTA) and system identification (SI), is given.

Distributed pressure sensing (DPS)

A fiber optics cable could be deployed with different sensors spaced in/along the well bore, i.e., a distributed sensor, capable of measuring parameters such as temperature, strain, acoustics and/or pressure along the well bore [5, 6]. Having an array of pressure measurements along the well could be used to estimate inflow from the reservoir and/or the flow rate in the well bore [7]. DPS is also used for reservoir parameter estimation, explained later below.

With multiple pressure measurements along the well bore, the pressure difference between two spatially distributed sensors can be calculated. The pressure difference consists of three main components, head loss, friction loss and, and acceleration loss. For a single-phase slightly compressible liquid the friction component primarily causes the pressure drop along a horizontal well. Based on the friction component the flow rate can be estimated in horizontal wells [1, 4]. In the case of deviated and vertical wells, there is a head loss component. With the relationship between the friction component of the pressure drop and the flow rate given in [8], the flow rate can be estimated for a given pressure drop due to friction, density, viscosity, pipe roughness, pipe diameter, the length, i.e., the sensor spacing.

Information about the zonal flow rate and the pressure gives the opportunity for reservoir parameter estimation [1, 9]. By estimating the flow rates and the pressure measurements during a PTA, system identification can be applied as done in [2] and [4] for reservoir parameter estimation. PTA using SI with spatially distributed pressure sensors is discussed next.

Pressure transient analysis (PTA) by use of system identification (SI)

Pressure transient analysis (PTA) is one of the essential diagnostic tools for a petroleum engineer which is used to predict future performance and to identify reservoir and well-bore properties [10]. An exploratory study showed the potential of applying system identification (SI) to analyze well test data [11]. Further research developed an SI framework which is partially used in this research; earlier research demonstrated the application of SI for PTA with numerical experiments and provided an extensive overview of the developments of PTA over the years [2]. Coupled reservoir-well bore simulations during a drawdown test with perfect measurements showed the possibility of estimating the permeability of layers in a box reservoir model with a high permeability patch [4].

SI is a widely technique in the process and control industry. SI is used to identify models or model parameters [12]. A change in the input, the flow rate, causes a pressure response which could be described by a system. The goal of applying SI is to increase understanding of the system, which is the reservoir and well bore in this case. So based on measurements, i.e., pressures and flow rates measured with DPS, model identification is possible.

The flow in the reservoir could be described with the radial flow equation for single-phase slightly-compressible liquids, which is solved in the Laplace domain with the Bessel functions, see [2, 4]. A causal structure can be determined by applying boundary conditions, as can been seen in Figure 2.1. The flow rate at the sand face, q_{sf}, could be calculated by,

$$q_{sf} = R_{11} q_e + R_{12} \Delta p_{sf}, \tag{1}$$

where R_{11} and R_{12} are transfer functions, which relate the flow rate q_{sf} to the flow rate at the boundary q_e and the pressure difference at the sand face Δp_{sf}. During a transient well test, the flow rate at the exterior boundary is assumed to be zero, and therefore we have

$$q_e = 0, \tag{2}$$

which leads to a direct relationship between Δp_{sf} and q_{sf} by transferfunctio R_{12},

$$q_{sf} = R_{12}\, \Delta\, p_{sf}. \tag{3}$$

The flow rate and pressure at the sand face should be known to use SI for PTA. Based on measurements the transfer function $R_{12,measured}$ can be approximated in the frequency domain, with e.g., the Matlab System Identification toolbox [13]. There is also an analytical solution for the transfer function based on the derivation of the radial flow equation, which will be explained in the method section. The analytical transfer function, depends on several reservoir parameters, such as porosity, permeability, compressability, viscosity, sensor spacing, well bore radius, exterior reservoir radius and skin [4]. $R_{12,analytical}$ could also be analysed in the frequency domain by subsituting the Laplace parameter s with $j\omega$.

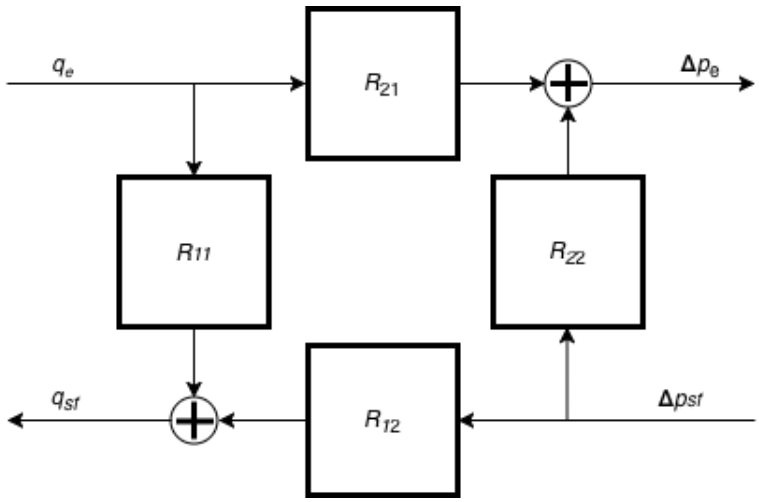

Figure 2.1: Causal structure describing the system dynamics; after [2].

Both transfer functions $R_{12,measured}$ and $R_{12,analytical}$ could be analysed in the frequency domain, which leads to the opportunity to make a visual comparison of the resulting frequency domain plots and use these for "manual" parameter estimation. This is done by calculating $R_{12,measured}$ based on q_{sf} and Δp_{sf}, and making realizations of $R_{12,analytical}$ based on prior information, and by varying the to-be-estimated parameter, e.g. permeability or, skin, trying to match the response of the two transfer functions.

3 Method

Due to the absence of real DPS data, synthetic pressure measurements are generated for the research described in this report. The synthetic well test for DPS is created with aid of a coupled well bore reservoir simulator. The Automated Differentiation General Purpose Research Simulator (AD-GPRS) is used [14] in this research. The choke diameter was added as well control by [3], which allows the testing with an arbitary (not necessarily piecewise constant) flow rate input signal which is one of the benefits of using SI [2]. The steps from making synthetic data all the way to interpretation of the PTA data with SI are given in a workflow described below.

3.1 Overview of workflow: Synthetic PTA with SI using DPS measurements

The workflow could be described in three main stages: (1) simulation of data, (2) data processing and (3) estimation of reservoir properties with SI, see figure 3.1. Synthetic well test data is created by simulation of a coupled well bore reservoir model. It is important to have an accurate description of the well bore for the data processing step. The output of the simulation are pressure and flow rate measurements along the well bore over time. A detailed description of the creation of synthetic data is given in the next section. Note, that in performing field experiments with DPS, no downhole flow rate measurements will be available, the flow rate needs to be estimated.

Data processing starts with pre-processing the pressure measurements over time. With additional information, such as the surface flow rate and/or choke diameter changes over time, the start of the transient flow regime can be estimated. The radial flow regime is identified which is a requirement for further SI analysis of the data. The flow rate inside the well bore can be estimated based on the pressure data, as will be explained in section 3.3. We note that PTA can be performed for build-up and drawdown well tests using the same underlying theory.

Having pressure data from the transient regime and the (estimated) zonal flow rates gives the opportunity to apply SI to estimate reservoir properties, such as the circumferentially averaged permeability, for each segment in the well. This is done by estimating a transfer function based on the processed measurements, i.e. the pressure and flow rates of an individual segment. Based on prior information an analytical transfer function can be constructed. The analytical and measured transfer function are compared to estimate reservoir parameters.

3.2 Generating synthetic PTA data

In this step of the workflow synthetic distributed pressure measurements are created with AD-GPRS based on a reservoir model. The pressure measurements of the segments inside the well bore will be used as inputs for the data processing steps. Requirements to create pressure transient data with the simulator are, (1) an accurate description of the well bore and the segments, i.e. with a multi segmented well bore model, (2) a refined grid around the well bore, (3) relative small time steps compared to those used in conventional simulation of reservoir performance.

The well bore in the model should be described with a Multi-Segmented Well (MSWell) model, which takes into account the pressure drop in the well bore over each segment; see Figure 3.4. The distributed pressure sensors in this research have a constant spacing inside the perforated zone. The well bore is modelled with the first segment having the tubing head pressure p_{tf} as input, with possibility of using the upstream pressure from the choke [3] as input instead of a fixed p_{tf}. The

effect of wellbore storage, due to compressibility in the well bore between the top of the reservoir section and the well head, can be accounted for by extending the well model to surface.

The dynamic reservoir model consist of grid and physical data. The grid data contain information about the grid cells, e.g. cell size, connection between cells, porosity, etc. The physical data contain information about the fluid properties and model formulation, e.g. black-oil, low enthalpy geothermal formulation, etc. To capture the effects of the transient pressure, the simulation grid needs to be refined near the well bore where converging radial flow leads to very hight flow velocities. Information about the grid and the physical data will be given before analysing the results of simulations.

Grids are constructed with the GMSH software package, which generates unstructured grids [15]. Unstructured grids are more flexible than regular (structured) grids and can therfore be used to, e.g., represent a complex well tractory or a strongly heterogeneous geological structure. An approach for constructing grids with a deviated well refined for PTA is explained by [16]. In this research we use a grid generation approach for deviated wells as explained in Appendix A. A difficulty with unstructured grids may arise for calculation of the well index, which defines the connectivity between the well and the reservoir grid [17]. In this research, this potential problem is mitigated by using hexahedrons for the grid blocks containing perforations of the well. As a consequence, the well index I_w can be calculated analytically according to [18]

$$I_w = 2\pi \frac{\sqrt{k_x k_y} h}{\ln\left(\frac{r_w}{r_o}\right)}, \tag{4}$$

where k_x and k_y are permeabilities in the *x* and *y* directions, *h* is the layer thickness, r_w is the well bore radius and r_o is the Peaceman radius which is given by

$$r_o = 0.2\Delta x, \tag{5}$$

where Δx is the grid block size. The version of the well index in represented in equation (5) is valid for a centered well in a regular rectangular grid. More complex formulation, using different geometrical factors, are typically used in irregular grids.

AD-GPRS is a connection-based simulator and requires the connection list (i.e. list with connections between two connected grid cells with the according transmissibility values) as input. Discretization in unstructured grids is more complicated due to the irregular shapes of the control volumes. Here the connection list is calculated with a discretizer developed in Python based on [14].

Simulation time steps and the well controls are required to simulate a reservoir model There is a marked difference between the typical time step size used for reservoir scale simulation (months to years) and those used for transient well testing: in order to create the transient pressure data, the time step should be sufficient small. The sampling time of the measurements is used to estimate the transfer functions, see Appendix B; the Matlab toolbox [13] only allows a fixed sampling time, thus the time step should be constant (at least during the radial flow regime).

The simulation of the dynamic coupled well-reservoir model gives information at each time step of the pressures and flow rates in each segment of the well bore. Having the flow rate data available from the simulation allows us to verify the implemented method (based on only pressures) for flow

rate estimation. One requirement of applying SI is to be in the radial flow regime. Flow rate estimation, measurement selection in the radial flow period and the pressure difference compared to steady state are discussed in the data processing step.

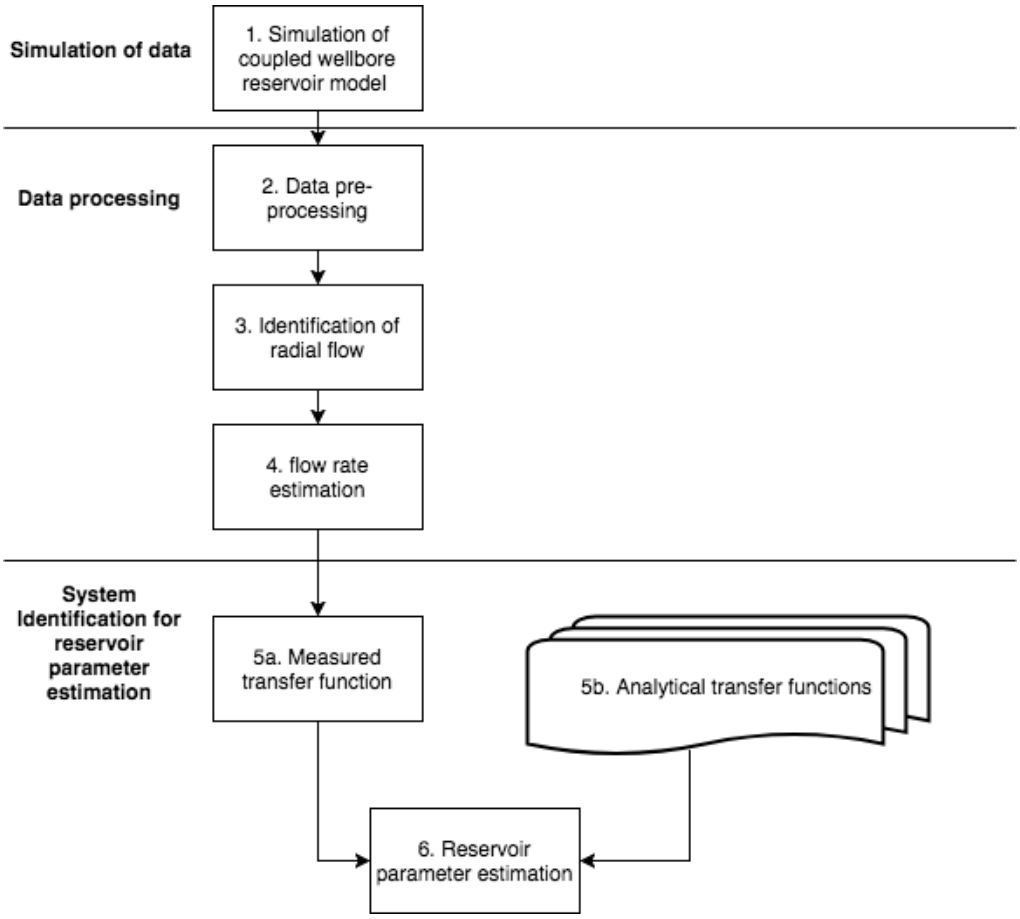

Figure 3.1: Workflow from creating synthetic PTA data to applying SI for parameter estimation.

3.3 Data Processing

Pressure measurements need to be processed in order to use them for parameter estimation with system identification. The data processing starts with extracting the well-test data from the measurements. This is followed by selecting the measurements during radial flow. The third step is to calculate the net inflow rate for each layer. With the pressure difference (compared to steady state) and the net inflow rate the transfer function can be estimated.

The data pre-processing (step 2, Figure 3.1) concerns mainly the selection of the specific moment in time where the well test actually starts, i.e. t_{start} in Figure 3.2. The well controls are important to know; in classical PTA, a constant flow rate is required. In this research the two different well controls used are a fixed surface flowrate; a fixed choke size. A change in surface flow rate or in choke size will result in a pressure response in the bottom hole pressure and will propagate through the reservoir, see Figure 3.2 which depicts a semi-steady-state situation (linearly declining reservoir pressure) followed by an exponential decrease in pressure as a result of changing the choke setting or the flow rate.

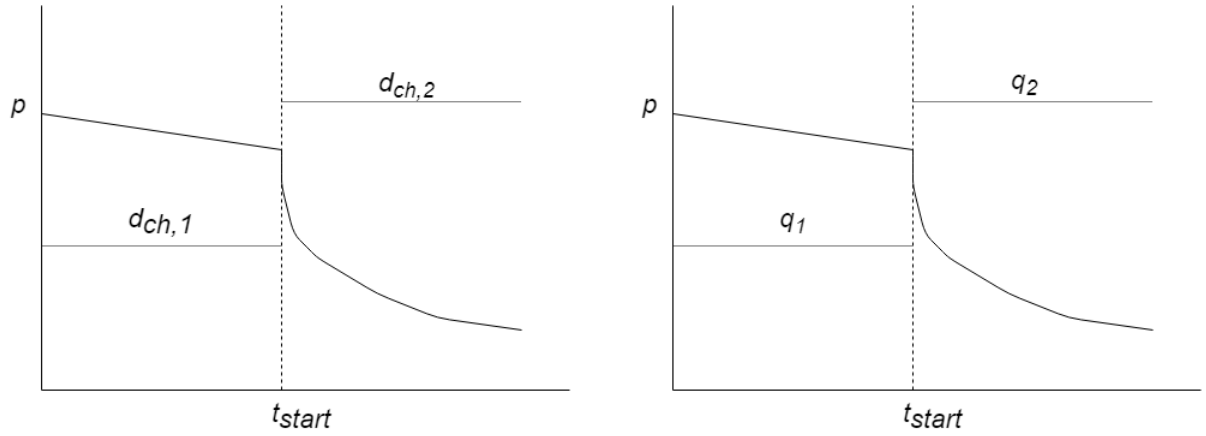

Figure 3.2 Fixed choke size (left) and fixed flow rate (right) as well controls, where the pseudo-steady state pressure decline changes into a transient regime at t_{start}.

Radial flow is a requirement for using SI for PTA. After the wellbore storage (WBS) effect, the flow in the reservoir behaves like infinite-acting radial flow. This flow regime can be identified with a straight line of the pressure derivative on the log-log scale [20]. The radial flow regime could be identified twice in horizontal and deviated wells; once early, i.e. just after a change in well setting, when the flow is radial toward the well bore, and once late, when the flow at larger distances is nearly radial towards the entire well. In-between a more complex transitional regime can be distinguished. In Figure 3.3 the difference between a well test for vertical and horizontal wells is displayed on a log-log scale. With the aid of the pressure derivative as seen in Figure 3.3, the pressure measurements during the radial flow period are selected which will be used for estimating the transfer function. In a deviated well the radial flow regimes will depend on the inclination of the well especially when a small reservoir height leads to a rapid effect of 'boundaries' (i.e. the top and bottom of the reservoir) on the pressure response.

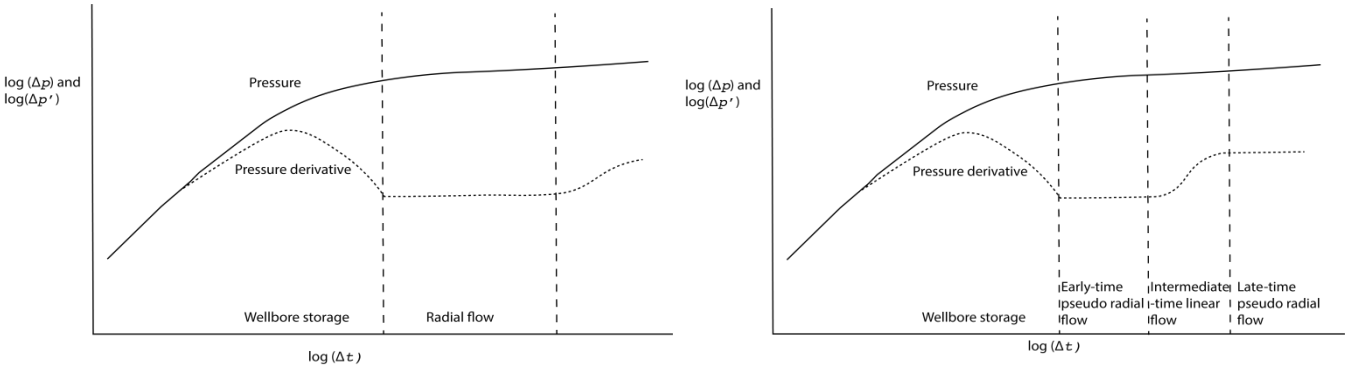

b Vertical well **b Horizontal well**

Figure 3.3 Pressure difference and pressure derivative in log-log scale for identification of the radial flow period.

The net inflow rate of a segment is required besides the pressure measurements for using SI. The flow rate of a segment can be estimated based on three pressure measurements. The first step is to obtain the flow rate at the interface between to segments. The pressure drop for a single phase liquid between two segments,

$$\frac{\mathrm{d}p}{ds} = \underbrace{\rho g \sin\theta}_{head\ loss} + \underbrace{\frac{\rho}{2d} f v|v|}_{friction\ loss} + \underbrace{\rho v \frac{dv}{ds}}_{acceleration\ loss}, \tag{6}$$

depends on the gravity (first term), friction (second) and acceleration component (last). The acceleration component is negligible for single-phase slightly compressible liquids [8], so equation (6) simply reduces to

$$\frac{\mathrm{d}p}{ds} = \underbrace{\rho g \sin\theta}_{head\ loss} + \underbrace{\frac{\rho}{2d} f v|v|}_{friction\ loss}, \tag{7}$$

where the head loss depends on the density ρ, the acceleration of gravity g, and pipe inclination θ. The friction loss depends on the diameter of the well d, the friction factor f and the velocity v. There is no pressure drop due to gravity in horizontal wells, but it could be computed if the density is known in vertical and deviated wells. The friction loss in terms of flow rate q instead of velocity v is,

$$\frac{dp}{ds}_{fric} = \frac{8\rho}{\pi^2 d^5} f q|q|. \tag{8}$$

The friction factor depends on ρ, q, d, viscosity μ and pipe roughness e. With the flow rate as the only unknown and the friction loss known, the flow rate can be estimated by minimizing the difference

$$R(q) = \frac{dp}{ds}_{fric,mes} - \frac{dp(q, f(q))}{ds}_{fric,calc}, \tag{9}$$

between the measured friction loss and the calculated estimated friction loss which depends on the flow rate. The calculated flow rate is at the interface between two pressure measurements. To calculate the net inflow rate of a certain segment, the flow rate at the top interface is subtracted from the flow rate at the bottom interface, see figure 3.4. Note, the (total) flow rate at the top of the first segment, i.e., the sensor at the top, is not calculated and therefore it is not possible to calculate the net inflow rate. The zonal flow rates are required for SI, and therefore parameter estimation is not possible for the first segment.

During field experiments the removal of measurement noise could be an important processing step. The pressure measurements in this research are created with an synthetic model and do not contain noise. The precision could be improved with measurement stacking as proposed for (near-) steady state flow [1], where the standard deviation of independent Gaussian-distributed zero-mean measurements errors is stacked to reduce the effects of random errors. In our case, stacking might not be practical: due to the transient behaviour the exact repetition of pressure transients to create multiple measurements will probably not be feasible.

Pressure and net inflow rate during the radial flow period are inputs for PTA with SI. The goal of the data processing step is to construct these inputs and this is done in three steps. The first is data pre-processing, the second step is to identify radial flow and the final step flow rate estimation.

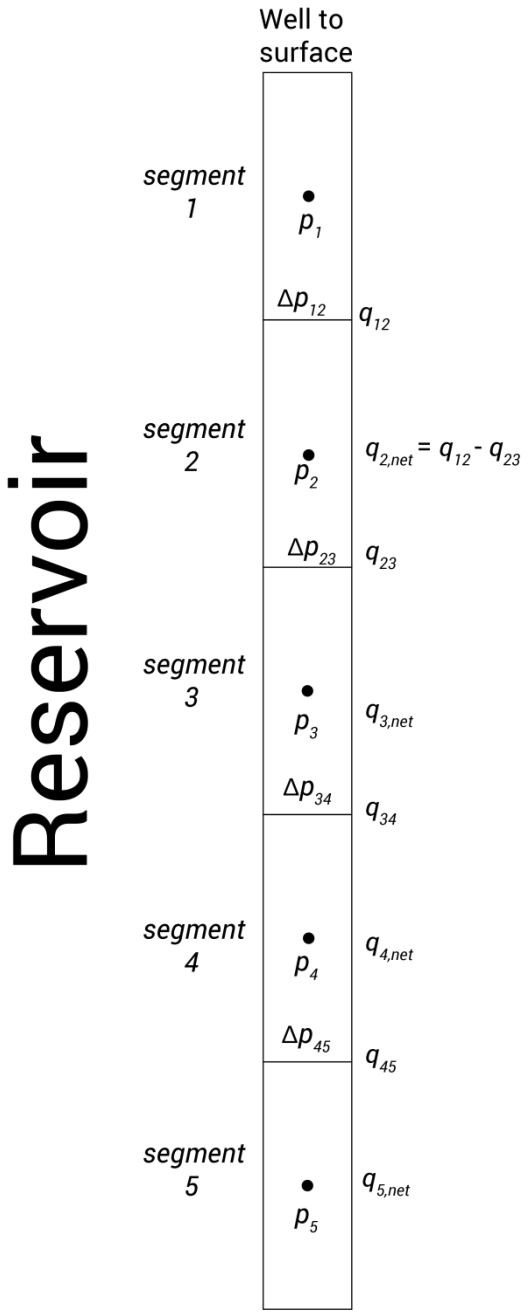

Figure 3.4 Example of an multi-segmented well modelled with five segments; each segment is perforated and has a pressure value. Based on the difference between the segment pressures, the flow rate at an interface is estimated.

3.4 Estimation of reservoir properties using System Identification

SI is used for PTA based on DPS data. In addition to date, SI requires a model, i.e. a mathematical relationship between an input and output, which is typically described by a set of transfer functions for specified boundary conditions, see Appendix C. As shown in figure 2.1 and equation 3, the transfer function R_{12}, is based on the net inflow rate q_{sf} and output p_{seg}. This transfer function can be estimated based on measurements which leads to $R_{12,mes}$ or can be calculated analytically based on prior information $R_{12,anl}$ (see Appendix C). The transfer functions are compared in the frequency domain.

The transfer function $R_{12,mes}$ is estimated with the Matlab System Identification toolbox [13]. A detailed description of how this toolbox is used is provided in Appendix B. The maximum frequency is restricted by the Nyquist Shannon frequency which is defined as half of the sampling frequency [21].

The analytical transfer function $R_{12,anl}$ depends on prior information about the model. The derivation of this transfer function is discussed in Appendix C. Realizations could be made based on different values of a chosen uncertain parameter. The addition of skin as uncertain parameter is discussed in [4]. The transfer function based on the Laplace parameter *s* is given by:

$$R_{12,anl}(s) = -\frac{2\pi kh}{\mu}\, r_e \sqrt{\frac{s}{\eta}}\frac{r_w}{r_e} \frac{I_1\left(r_w\sqrt{\frac{s}{\eta}}\right)K_1\left(r_e\frac{\sqrt{s}}{\eta}\right) - K_1\left(r_w\sqrt{\frac{s}{\eta}}\right)I_1\left(r_e\frac{\sqrt{s}}{\eta}\right)}{I_1\left(r_e\sqrt{\frac{s}{\eta}}\right)K_0\left(r_w\frac{\sqrt{s}}{\eta}\right) + I_0\left(r_w\sqrt{\frac{s}{\eta}}\right)K_1\left(r_e\frac{\sqrt{s}}{\eta}\right)}, \tag{10}$$

where *I* and *K* are Bessel functions, r_e is the external reservoir boundary (assuming a circular reservoir), *k* is the permeability, *h* is the segment length and η is the hydraulic diffusivity,

$$\eta = \frac{k}{\phi\mu c_t}, \tag{11}$$

with porosity ϕ, the total compressability c_t and viscosity μ. $R_{12,anl}$ could also be analyzed in the frequency domain by subsituting the Laplace parameter s with $j\omega$.

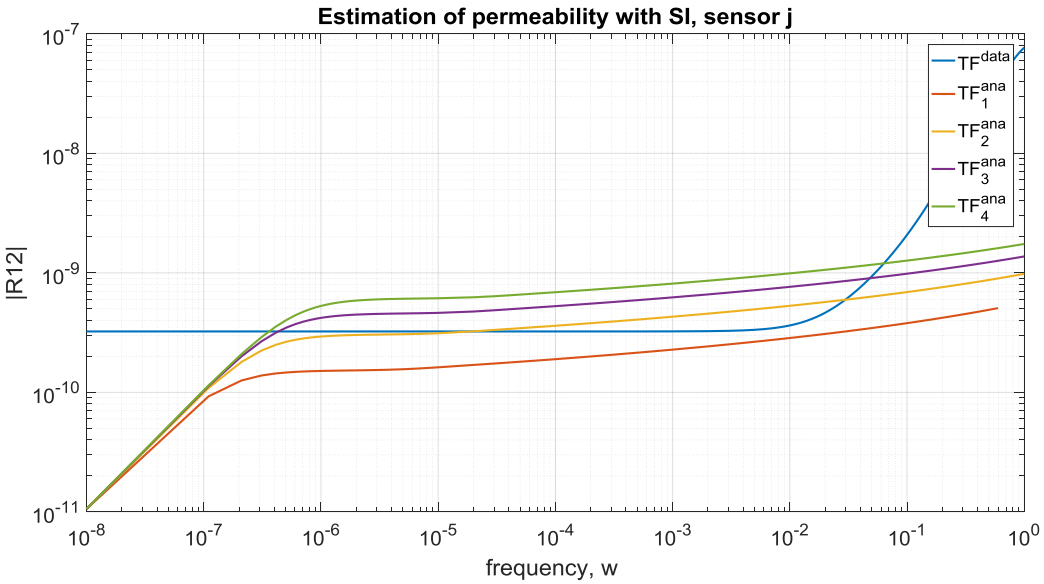

Figure 3.5 Parameter estimation for a well segment by matching the transfer function, TF^{data}, with realizations of the analytical transfer function. Note, the match is only observed within a certain frequency range.

Parameters are estimated by matching the different transfer functions with different realizations of the analytical transfer function, i.e. by varying the to-be-estimated parameter until an acceptable match is obtained. The parameter estimation step is done for each segment separately. See Figure 3.5 for an example of parameter estimation in the frequency domain for a segment.

4 Numerical experiments for parameter estimation with SI in a vertical well

Three numerical experiments are performed with a coupled wellbore-reservoir simulator to create synthetic DPS data for a vertical well. With the synthetic DPS data the flow rate is estimated and the permeability is estimated with SI with the workflow described in Chapter 3.

4.1 Numerical experiments

The three types of numerical experiments are based on a homogenous, a layered and a heterogeneous reservoir (where homogeneity refers to the permeability only). All the steps of the workflow are explained with the first experiment with the homogenous reservoir. In the second experiment heterogeneity is added to the reservoir by assigning different permeability values to the layers in the reservoir. Finally a heterogeneous reservoir is used to create the synthetic well test data.

The experiments are performed with a cylindrical reservoir model with a vertical production well with twenty pressure sensors. The specifications of the model can be found in Appendix A. Only the permeability and well indices of the perforations are changed for the three types of numerical experiments. A drawdown test with a constant production rate is done in all the numerical experiments described in this chapter.

4.2 Using SI to identify reservoir properties in a homogenous reservoir

The workflow described in Chapter 3 is used to create synthetic data. In the simulation a drawdown test is performed with a constant flow rate. The well test starts after two days, which can be observed in Figure 4.1. The available measurements are the tubing head pressure, surface flow rate and the downhole pressures. Homogenous reservoirs are used with permeabilities of 50, 100, 150 and 200 mD respectively.

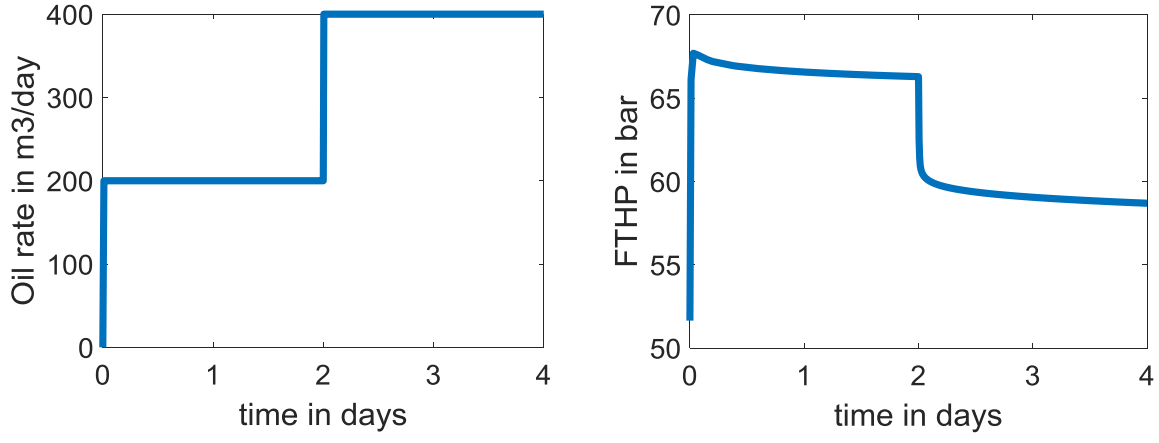

a) Oil rate as well control b) Tubing head pressure

Figure 4.1 Oil rate and pressure response during drawdown well test. The pressure data used for PTA is after 2 days.

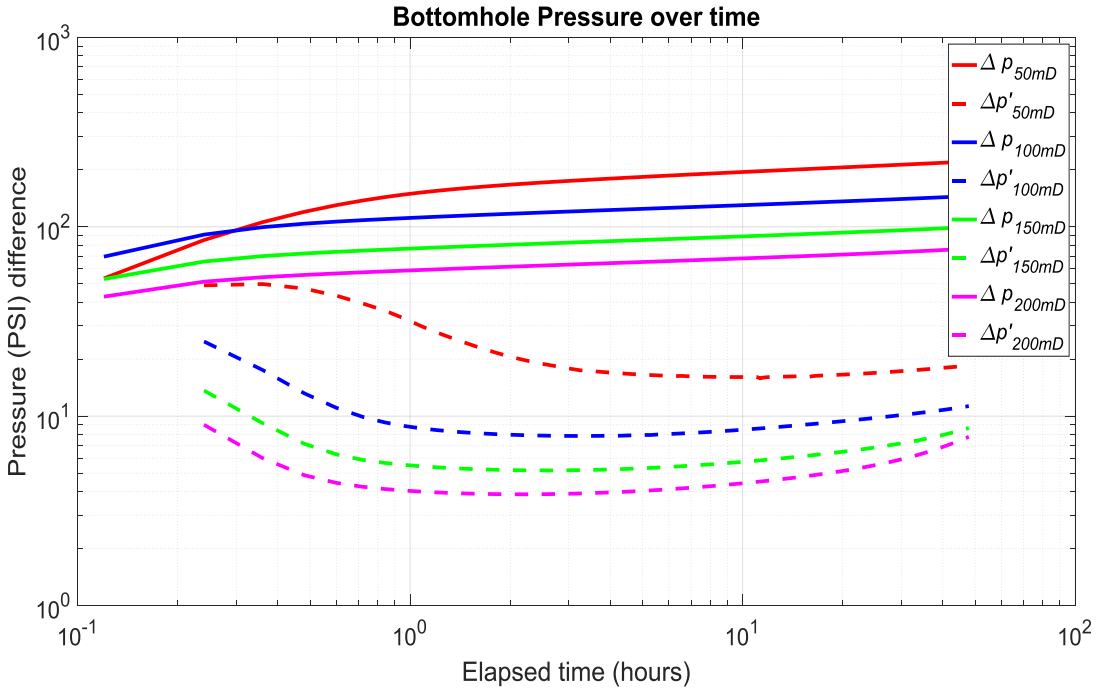

Figure 4.2 Diagnostic plot with pressure difference and derivative of pressure difference for 50, 100, 150 and 200 mD.

In the pre-processing step of the workflow, the pressure difference is calculated based on the pressure at two days and subtracting the measurements after the start of the well test. The calculation of the pressure derivative and pressure difference are plotted in the diagnostic plot given in Figure 4.2. The figure shows that the radial flow period is different for each permeability. Different pressure measurements need to be selected to analyse with SI, due to the requirement of radial flow. The well-bore storage effect is not visible at the start of the plot due a relatively large time step.

The next step is estimation of the net flow rate of each segment of the well bore. Figure 4.3 shows the process of flow rate estimation. In Figure 4.3a, the calculated pressure drop due to friction along the well is compared with the results from the simulation of AD-GPRS. Note that the friction at the bottom of the well is low compared to the top due the increasing flow rate. With the friction component of the pressure drop calculated, the flow rate at the segment interfaces can be calculated, as shown in Figure 4.3b. The flow rate for the top interface of the highest segment, which in this case is at a depth of 2000 m, is not calculated because there is no pressure measurement available above the highest segment. The total flow rate for the other segment interfaces aligns with the results obtained from the simulator. The net flow rate for a homogenous reservoir should be approximately the same, which is shown in Figure 4.3c. Only the two bottom zonal flow rates are not accurate compared to the other estimates because of the very low flow rates in these zones which result in higher (relative) errors . Figure 4.4 provides a comparison between the estimated flow rate based on DPS measurements and the flow rates from AD-GRPS.

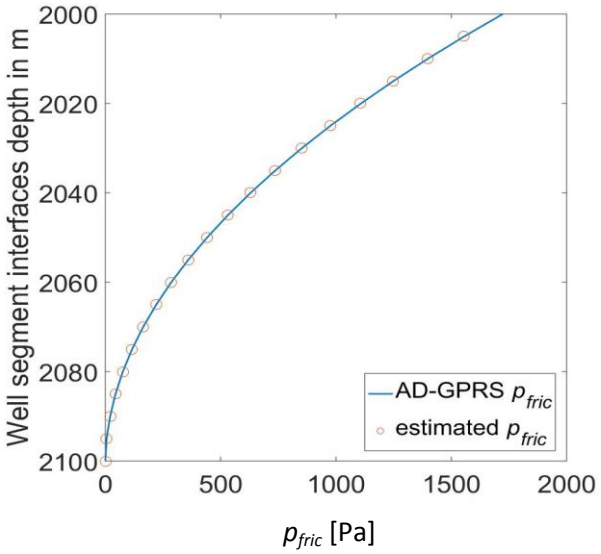

a) Pressure drop due to friction along borehole

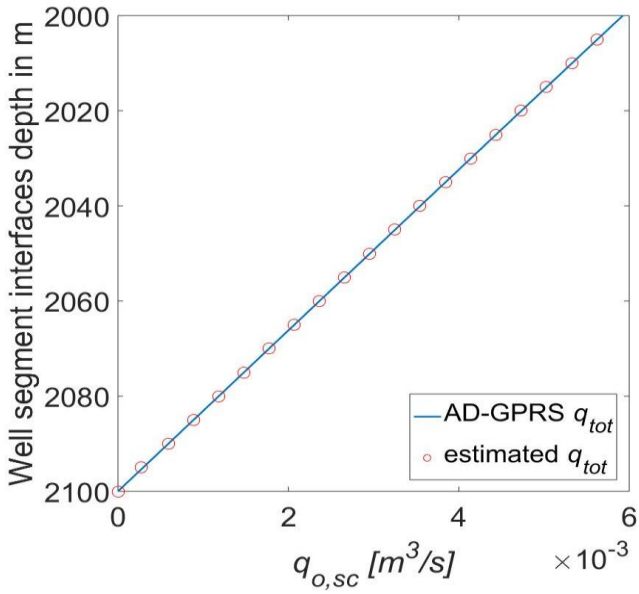

b) Total flow rate

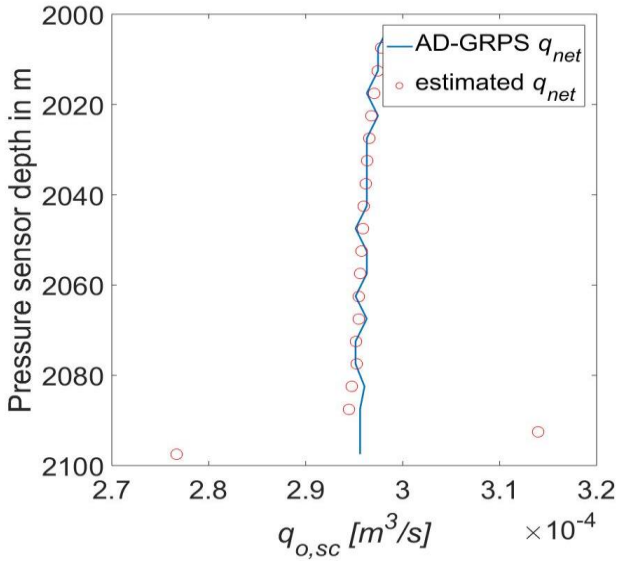

c) Net flow rate

Figure 4.3 Flow rate estimation of 100 mD homogenous reservoir analysed at t = 4.28 hours.

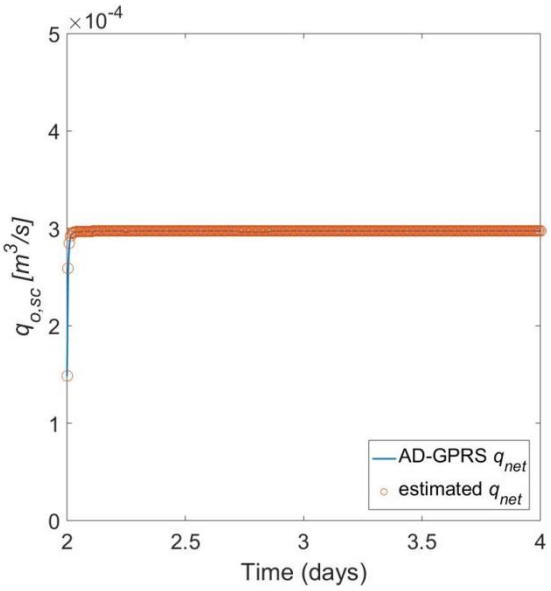

a) inflow rate at 2012.5m (sensor 3)

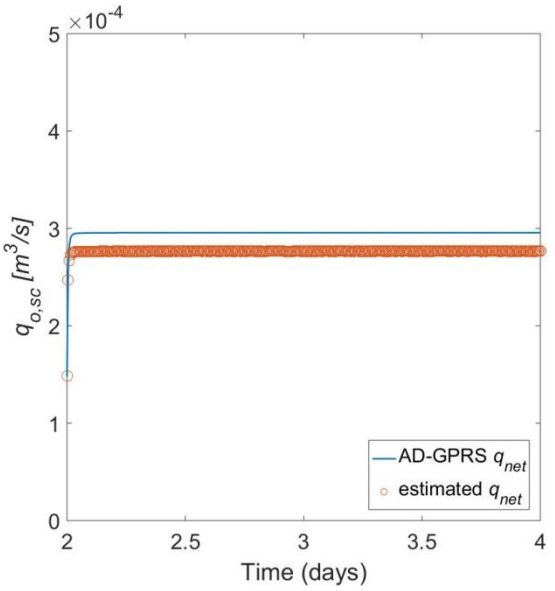

b) inflow rate at 2097.5m (sensor 20)

Figure 4.4 Segment net flow rate comparison between estimated flow rate and flow rate from AD-GPRS.

The transfer function based on data is estimated with the net flow rates and pressure measurements of a certain segment. In Figure 4.5 the transfer function based on the data for a homogenous reservoir of 100mD is compared with four analytical transfer functions. The permeability can be estimated for the 100mD homogenous reservoir within a certain frequency range.

The goal of parameter estimation with SI with the DPS is to estimate averaged production parameters along the well bore. Figure 4.4 and Figure 4.5 showed flow rate estimation and parameter estimation for two pressure sensors. In Figure 4.6, a permeability profile along the well bore is displayed for the homogenous reservoir with permeabilities 50, 100, 150 and 200 mD. The permeability for 100mD, as seen in Figure 4.6b, shows that the permeability can be estimated with SI. The results for 50mD are worse because the low permeability leads to low flow rate which can be less well estimated (because of higher relative errors). A general trend can be observed that the estimated values at the lower sensors deviate more compared to the estimation at the top.

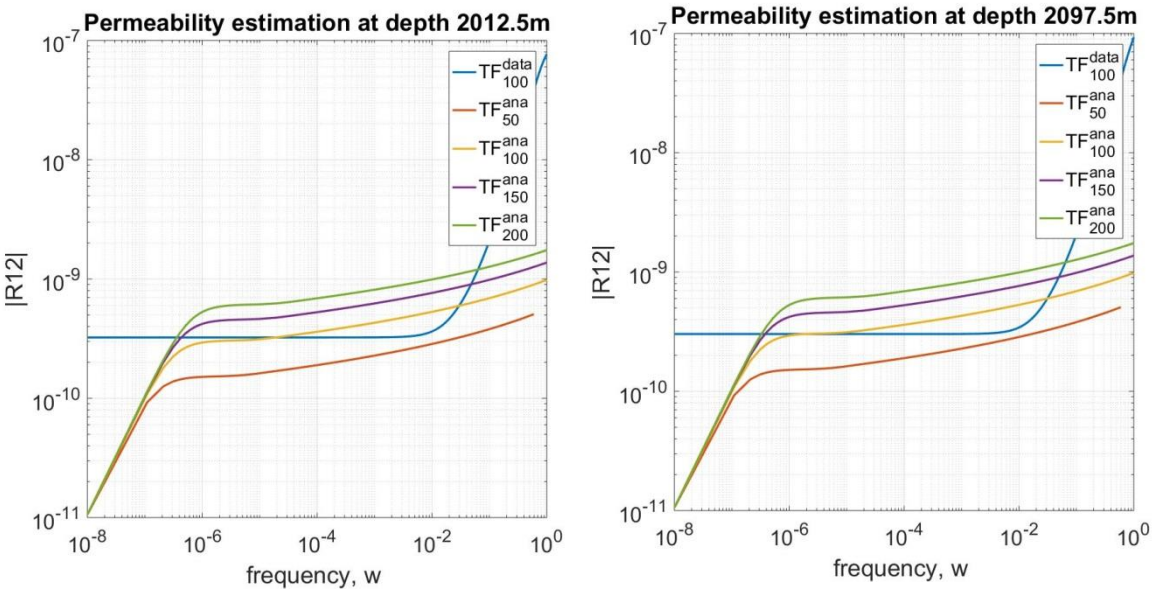

a) Sensor depth 2012.5m

b) Sensor depth 2097.5m

Figure 4.5 Estimation of permeability at depths 2012.5m and 2097.5m. The blue curve is the estimated transfer function based on the data. The other curves are realizations based on different permeability values.

4.3 Using SI to identify reservoir properties in a layered reservoir

In this experiment the permeability in two layered reservoir is estimated with synthetic well test. The first layered reservoir has primarily layers of 100 mD, with in between layers of 30 mD and layers of 300 mD. The second reservoir has layers with permeability of 500 mD, and a few layers of 10 mD and 100 mD, see Figure 4.6 for a cross section of the reservoir. The goal of this experiment is to see if the heterogeneity in permeability could be recognised with SI. The same steps from the workflow and the homogenous reservoir are applied to get final results shown in Figure 4.7 and from it can be concluded that the heterogeneity can be estimated with SI. Figure 4.8, shows the estimated flow rates for layers with different flow rates are accurately estimated.

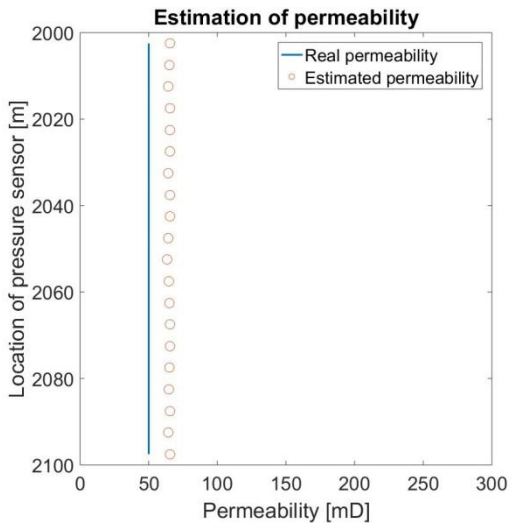

a) Homogenous 50 md

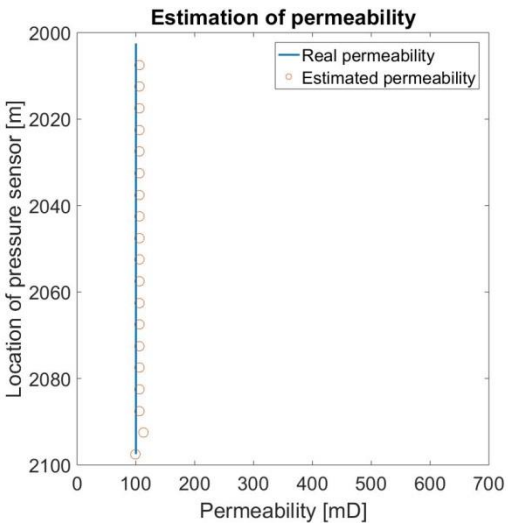

b) Homogenous 100 md

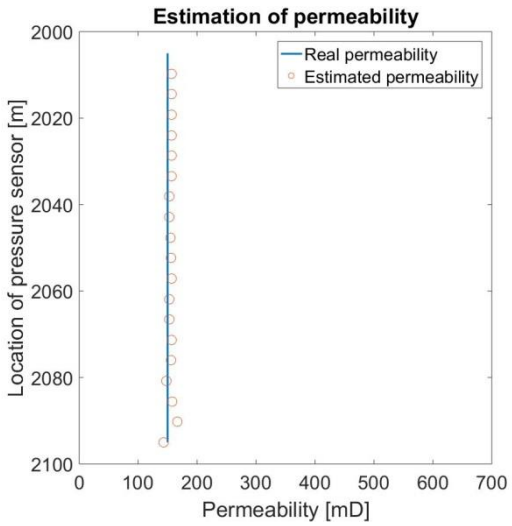

c) Homogenous 150 mD

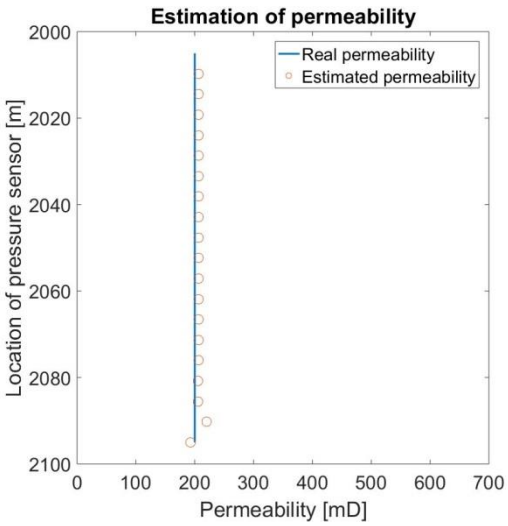

d) Homogenous 200 mD

Figure 4.6 Estimation of permeability in a vertical well homogenous reservoir with DPS based on SI.

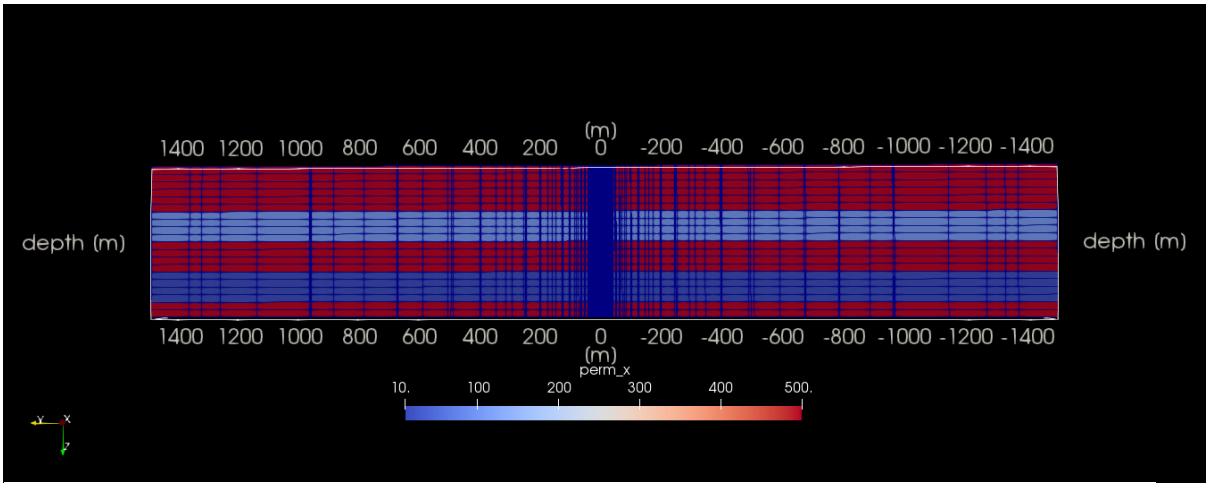

Figure 4.7 Cross section of the reservoir grid, with the production well at 0 m, layered reservoir 2.

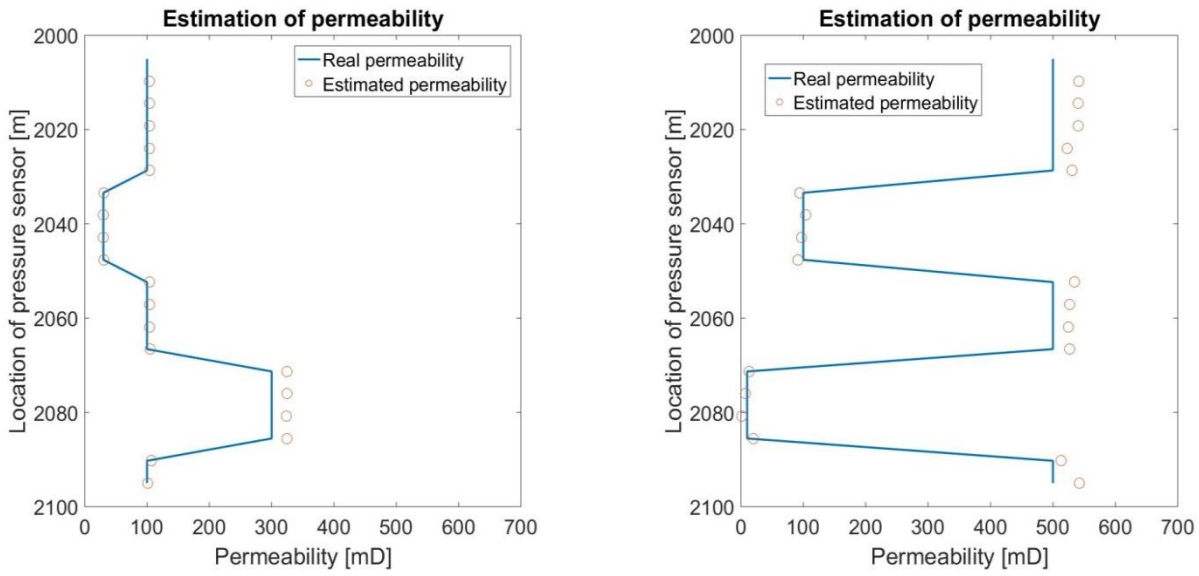

a) Layered reservoir 1

b) Layered reservoir 2

Figure 4.8 Estimation of permeability in layered reservoir with DPS based on SI

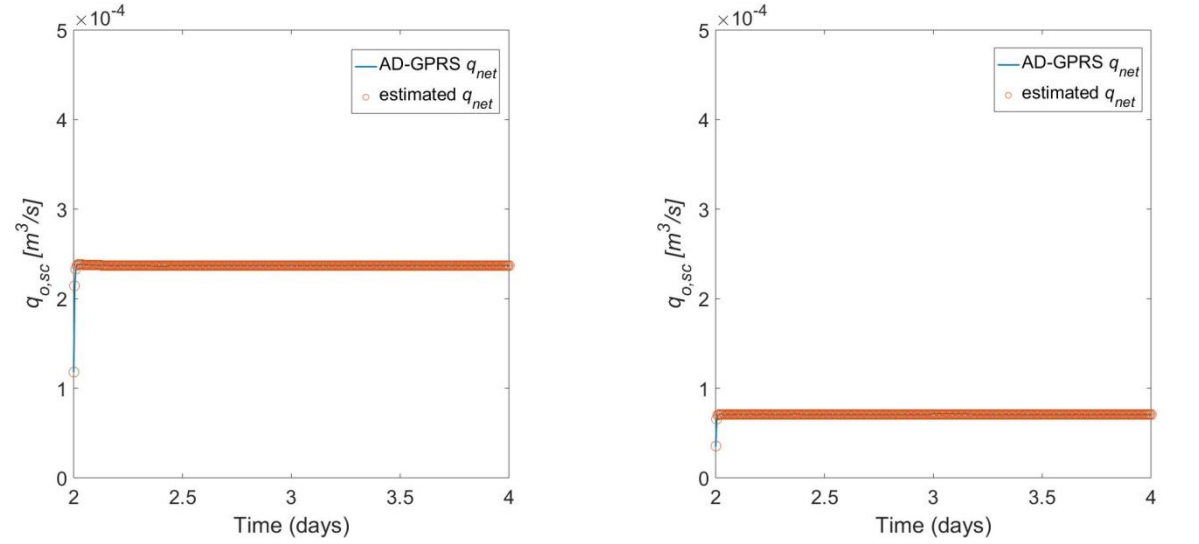

a) Sensor 3, depth 2012.5m – 100mD

b) Sensor 8, depth 2037.5m – 30mD

Figure 4.9 Estimation of flowrate in layered reservoir of layers with different permeabilities for layered reservoir 1.

4.4 Using SI to identify reservoir properties in a heterogeneous reservoir

In this numerical experiment a permeability field is extracted from Petrel and mapped on the unstructured grid defined in Appendix A. The permeability field is based on the porosity-permeability relationship observed in the Delft sandstone [22]. The transmissibility is calculated with the developed Python based TPFA discretizer which can handle heterogeneity and unstructured grids. The well index is calculated based on the permeabilities in the well grid block. Parameter estimation with SI gives circumferentially averaged permeabilities based on the flow rate and the pressure

response. Thus, in this case, it is not possible to verify the results. A selection of permeability fields is visualized and compared to the estimated permeability obtained from SI.

The low permeability estimates at 2037.5m and 2077.5m, and the high permeability estimates obtained at depths 2057.5, 2087.5m are investigated. Figure 4.10 shows that low and high estimated permeabilities from Figure 4.11 correspond to the permeabilityfield of those specified layers.

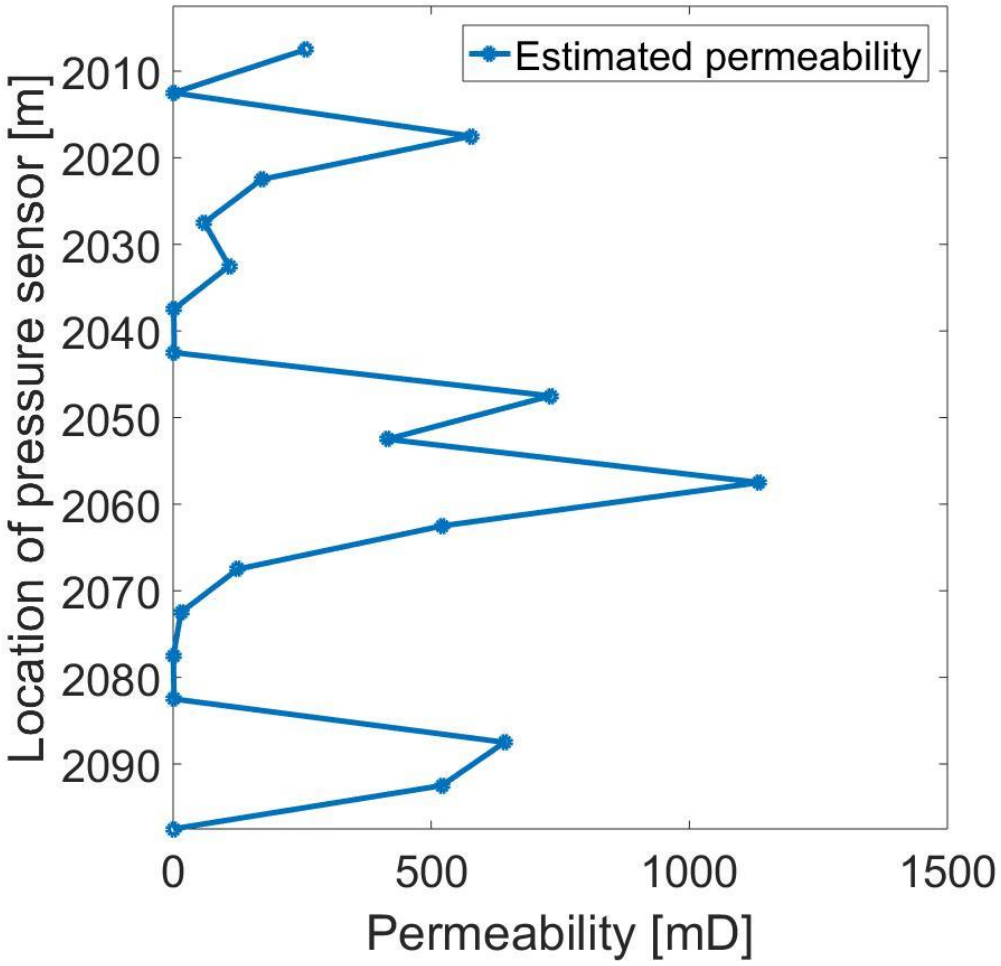

Figure 4.10 Permeability estimate of the heterogeneous model.

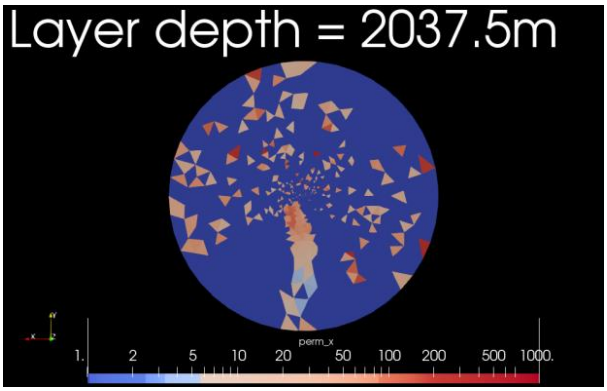

a) Layer 8

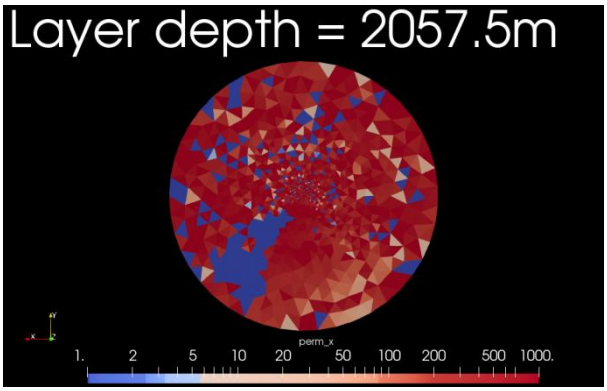

b) Layer 12

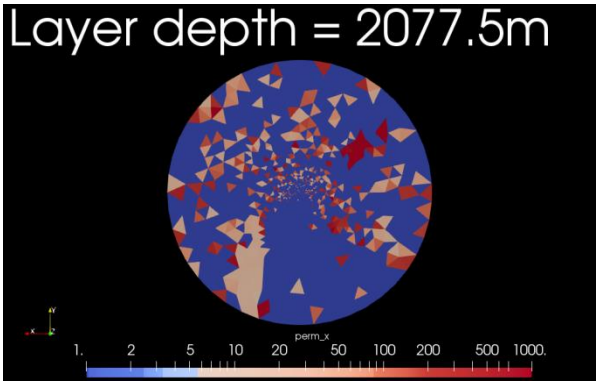

c) Layer 16

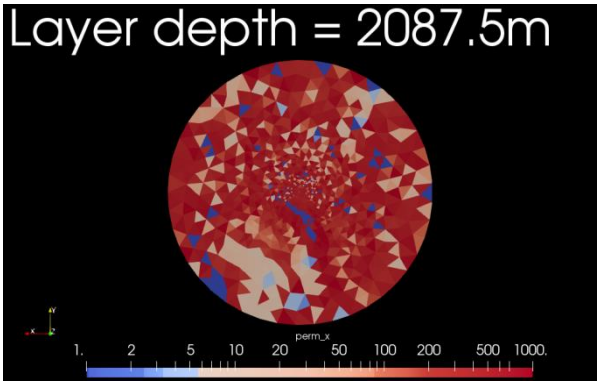

d) Layer 18

Figure 4.11 Estimation of permeability in a vertical well heterogeneous reservoir with DPS based on SI

5 Numerical Experiments for parameter estimation with SI in a deviated well

The next step in this research is to model a deviated well, which increases the complexity of the reservoir grid. A deviated well bore with an inclination of 45 degrees is modelled. The main challenge was grid refinement around the well bore, see Appendix A. A layered reservoir is investigated in this chapter.

5.1 Setup of numerical experiments

The numerical experiments in this chapter are performed by doing PTA with an implemented choke model which implies that the flow rate is not constant during the transient period.

An experiment with a heterogeneous layered reservoir is performed in this chapter. The workflow described in Chapter 3 is used to estimate the permeability with SI during PTA for DPS. The influence of measurement errors is investigated.

5.2 SI for PTA with a deviated well in a layered reservoir

Instead of changing the flow rate the choke diameter is changed, to mimic a realistic production scenario, see Figure 5.1. After two days the choke diameter is changed which marks the start of the well test. The flow rate is assumed to be unknown and will be estimated and compared to the output of AD-GPRS.

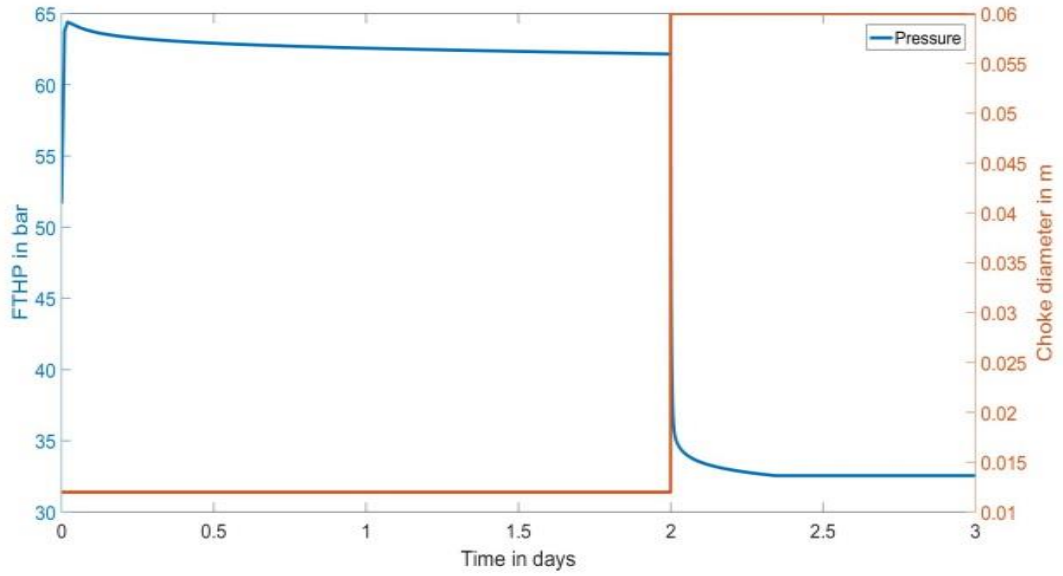

Figure 5.1 Flowing tubing head pressure (FTHP) response and choke size during drawdown well test. The pressure data used for PTA is after 2 days. The flow rate is not constant.

The diagnostic well test plot, Figure 5.2, shows that the radial regime is identified. However, there are no signs of intermediate linear flow, which can be expected in horizontal wells.

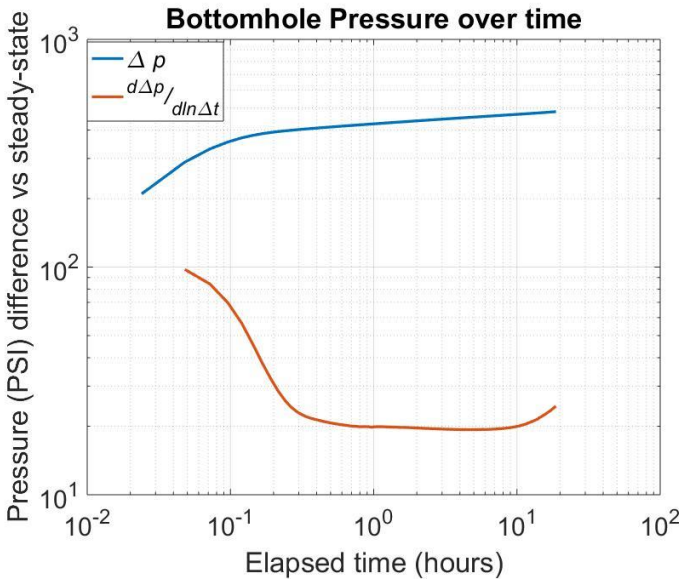

Figure 5.2 Typical diagnostic plot with pressure difference and derivative of pressure difference. .

The flow rate is estimated with the same procedure explained in Chapter 3 and applied in Chapter 4. Note, that the difference in terms of depth and the difference between two well segments is not equal to each other in deviated wells. The estimated net flow rate at segment 10 is plotted in Figure 5.3; the flow rate is not constant due to the implementation of the choke as the well control.

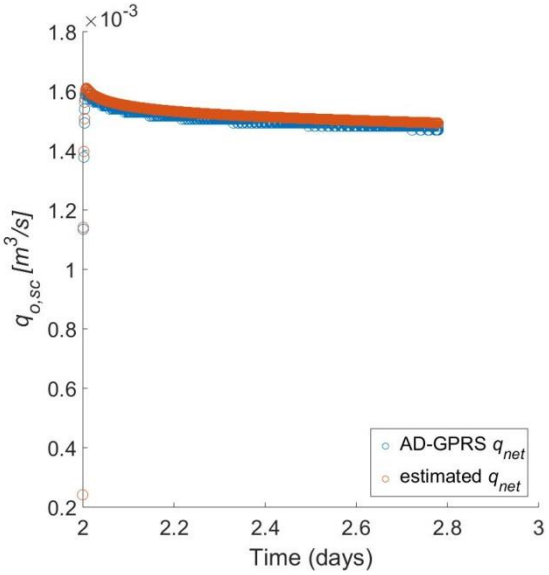

Figure 5.3 Flow rate estimation

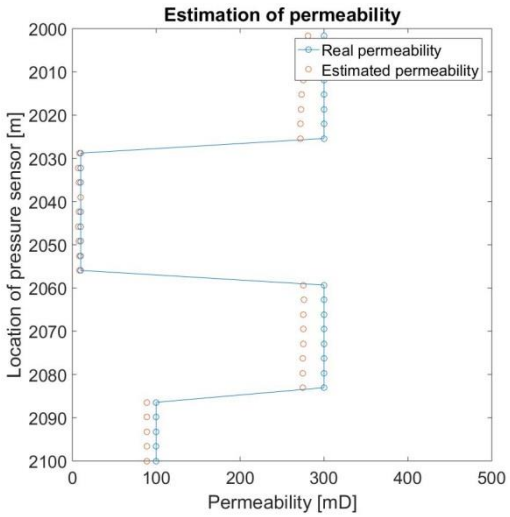

a) No error

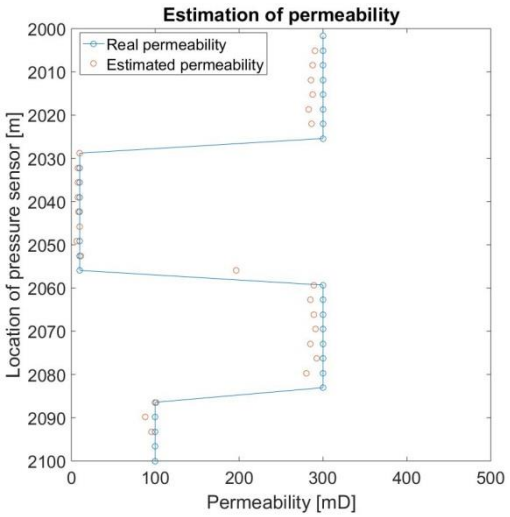

b) 10 Pa

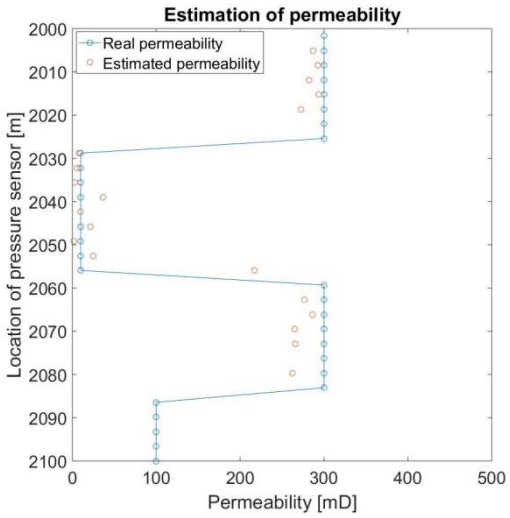

c) 100 Pa

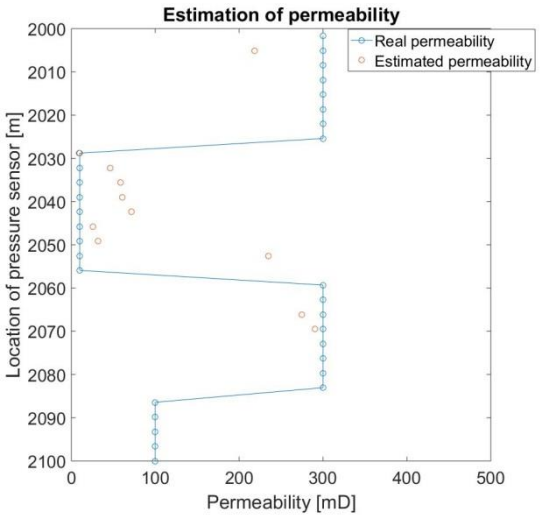

d) 1000 Pa

Figure 5.4 Effect of measurement errors on estimation of permeability in a deviated well heterogeneous layered reservoir.

Figure 5.4 shows the effect of measurement noise on the estimation of the permeability with SI. Noise has more effect on the estimated permeability at the bottom of the reservoir. This is because the flow rate estimate depends on the pressure difference between two segments, and near the bottom of the well the flow rate is lower. The estimated permeability does follow the trend but does not match the modelled permeability exactly, see Figure 5.4a. A possible explanation is that the well index is not calculated accurately for the deviated wells, and further research into this aspect is recommended.

6 Conclusions

The focus of this research is to investigate the scope for application of system identification (SI) as pressure transient analysis (PTA) method using distributed pressure sensors (DPS). Testing SI as a new procedure for well testing is done with numerical experiments using synthetic data due to the absence of real data. In this research a detailed workflow is explained with steps to construct synthetic examples, process the well test data, estimate the flow rate of each individual layer, and analyse the pressure and flow rate data with SI to identify reservoir properties.

Results obtained from a well test of a vertical well in a homogenous reservoir show that the net inflow rate and permeability of the reservoir can be estimated with SI. The next experiment was to identify heterogeneities in a layered reservoir were the different permeabilities can be identified with SI. The last vertical-well experiment was to estimate the permeability for a heterogeneous reservoir. Qualitative validation of the permeability results is not possible, due to the heterogeneity and flow paths, etc.; however the permeability field of a layer matched visually with the estimated (average) permeability.

The final experiment was performed with a deviated well in a layered reservoir and illustrated that the flow rate can be estimated. A reasonably accurate estimate of the permeability was obtained in the experiments, with errors likely due to the way the well index is calculated. Measurement errors influence the parameter estimation process in both inputs for SI: (1) the measure pressures are less accurate, (2) and therefore also the estimated flowrates are less accurate.

Acknowledgement

This research was carried out within the context of the ISAPP Knowledge Centre. ISAPP (Integrated Systems Approach to Petroleum Production) is a joint project of TNO, Delft University of Technology, ENI, Statoil and Petrobras.

References

[1] F. Farshbaf Zinati, J.-D. Jansen, and S. M. Luthi, “Estimating the specific productivity index in horizontal wells from distributed-pressure measurements using an adjoint-based minimization algorithm,” *SPE Journal,* vol. 17, no. 03, pp. 742-751, 2012.

[2] M. Mansoori, P. Van den Hof, J.-D. Jansen *et al.*, “Pressure-Transient Analysis of Bottomhole Pressure and Rate Measurements by Use of System-Identification Techniques,” *SPE Journal,* vol. 20, no. 05, pp. 1,005-1,027, 2015.

[3] R. N. Moghaddam, *Implementation of Choke Models into the AD-GPRS*, Delft University of Technology, 2017.

[4] R. N. Moghaddam, *Model development for Physical Parameter Estimation of Horizontal Well using Drawdown Data*, Delft University of Technology, 2017.

[5] A. H. Hartog, *An introduction to distributed optical fibre sensors*: CRC Press, 2017.

[6] D. A. Krohn, T. MacDougall, and A. Mendez, *Fiber optic sensors: fundamentals and applications*: Spie Press Bellingham, WA, 2014.

[7] F. Farshbaf Zinati, “Using Distributed Fiber-Optic Sensing Systems to Estimate Inflow and Reservoir Properties,” TU Delft, Delft University of Technology, 2014.

[8] J.-D. Jansen, *Nodal Analysis of Oil and Gas Production Systems*: Society of Petroleum Engineers, 2017.

[9] C. Beokhaimook, “Quantifying Near-Wellbore Permeability Heterogeneity Using Wellbore Flow Modeling and Fiber Optics Distributed Pressure Sensor,” Colorado School of Mines. Arthur Lakes Library, 2018.

[10] M. M. Kamal, “Transient well testing,” *SPE Monograph,* vol. 23, 2009.

[11] I. Kuiper, “Well Testing in the Framework of System Identification,” 2009.

[12] L. Ljung, "System identification," *Signal analysis and prediction*, pp. 163-173: Springer, 1998.

[13] Matlab, "System Identification Toolbox," Matlab, ed., Mathworks, 2017.

[14] D. Voskov, Y. Zhou, and O. Volkov, “Technical description of AD-GPRS,” *Energy Resources Engineering, Stanford University*, 2012.

[15] C. Geuzaine, and J. F. Remacle, “Gmsh: A 3-D finite element mesh generator with built-in pre- and post-processing facilities,” *International journal for numerical methods in engineering,* vol. 79, no. 11, pp. 1309-1331, 2009.

[16] V. Artus, D. Fructus, and O. Houzé, "Simulation of Deviated Wells Using 3D Unstructured Grids of Flexible Resolution."

[17] L. Li, D. Voskov, J. Yao *et al.*, “Multiphase transient analysis for monitoring of CO2 flooding,” *Journal of Petroleum Science and Engineering,* vol. 160, pp. 537-554, 2018.

[18] D. W. Peaceman, “Interpretation of Well-Block Pressures in Numerical Reservoir Simulation With Nonsquare Grid Blocks and Anisotropic Permeability,” *Society of Petroleum Engineers Journal,* vol. 23, no. 03, pp. 531-543, 1983/6/1/, 1983.

[19] M. Karimi-Fard, and L. J. Durlofsky, “A general gridding, discretization, and coarsening methodology for modeling flow in porous formations with discrete geological features,” *Advances in water resources,* vol. 96, pp. 354-372, 2016.

[20] D. Bourdet, J. Ayoub, and Y. Pirard, “Use of pressure derivative in well test interpretation,” *SPE Formation Evaluation,* vol. 4, no. 02, pp. 293-302, 1989.

[21] M. H. Weik, "Nyquist theorem," *Computer Science and Communications Dictionary*, pp. 1127-1127, Boston, MA: Springer US, 2001.

[22] J. H. Groot, “The Role of Reservoir Geology and Reservoir Architecture on Geothermal Doublet Performance,” University of Utrecht, University of Utrecht, 2014.

Appendix A. Modelling of a well-test for a vertical well

An unstructured grid is created in GMSH with refinement around the well, see Figure A.1. In Table A.1, the model parameters are given for creating synthetic PTA data with AD-GPRS.

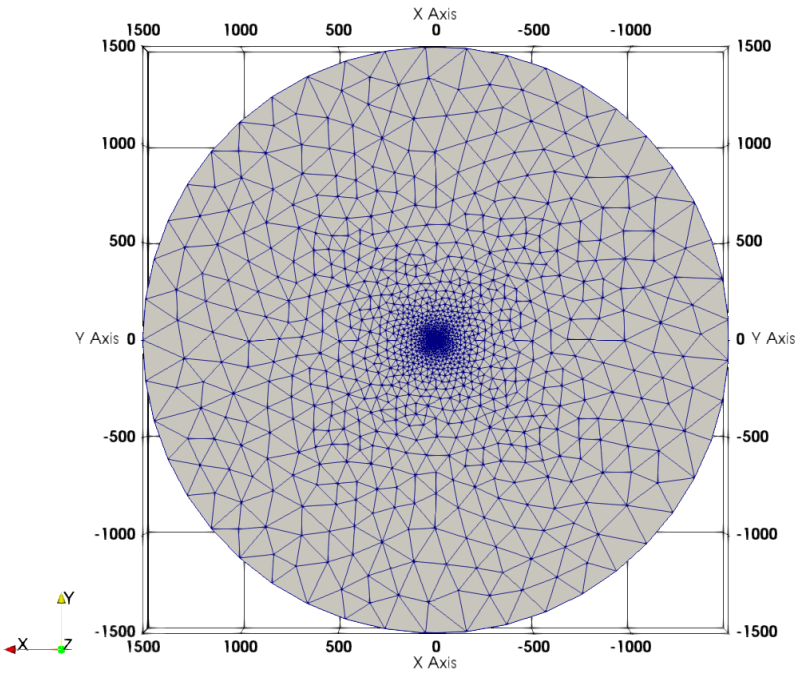

Figure A.1 Top section of an unstructured radial grid, with refinement around the well bore. This grid is used for the simulations of chapter 4.

Table A.1: Model parameters for the vertical well test case.

Model properties	SI Units
Reservoir boundary	1500 m
Well radius	0.3048 m
Reservoir thickness	100
Pipe internal diameter	0.0727
Well length	2000 meter
Permeability	Specified per model
Porosity	0.20
Dynamic viscosity	$1.2\ 10^{3}$ Pa s
Total compressibility	$1.5\ 10^{-10}$ 1/Pa

Skin	0
Number of segments in completed zone	20
Segment length	5 m
Height of completed zone inside of segment	5 m

Modelling a deviated well with refinement around the well bore, and specified well segments, i.e. to mimic the DPS data, was done in GMSH. The grid is created in three steps. The first step is to create an empty deviated cylinder with an inclination, this geometry will be filled with hexahedrons with a constant spacing between them. This is needed to ensure a constant well segment length, for implementation of the MSwell model and easy calculation of the well index. The second step is to add a small box around the cylinder, i.e. a near well-bore area. To ensure the well is connected to this second volume, the mesh is filled with prisms, see Figure A.2 and A.3. Finally an outer layer of tetrahedrons is added.

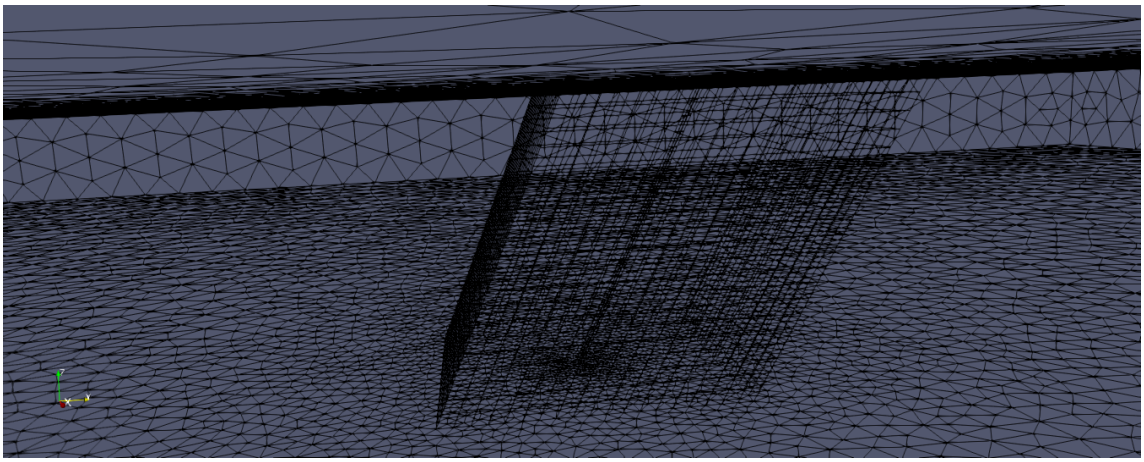

Figure A.2: Wireframe of the near well bore area, with the well visible inside.

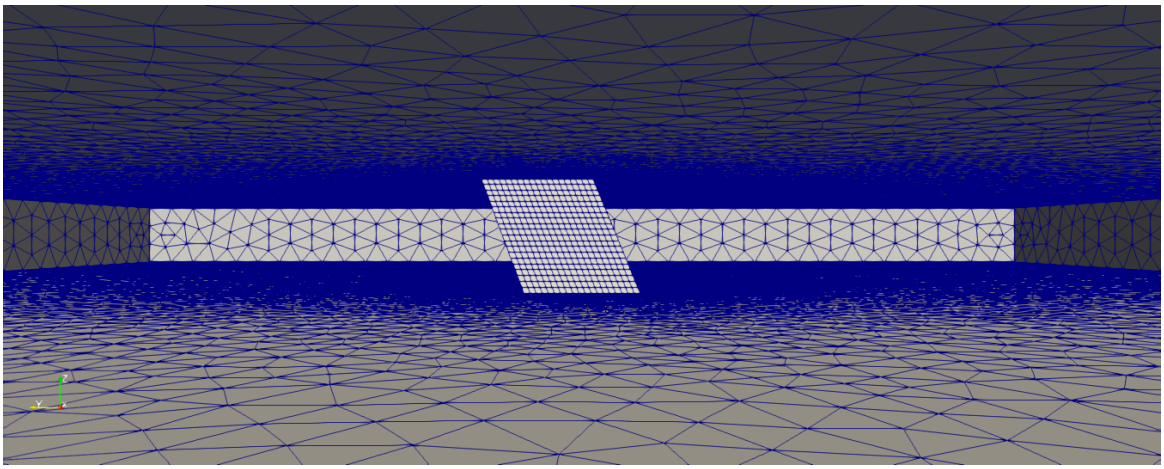

Figure A.3: Screen shot of near well bore area inside of the reservoir mesh.

Appendix B. System Identification Toolbox in Matlab

The 'measured' transfer function, is a transfer function estimated based on the measurements with the aid of the SI toolbox in Matlab. There are two methods to use the System Identification toolbox:

1. use the SystemIdentification app and,
2. use commands of the SystemIdentification toolbox, for detailed instructions refer to [12].

The first step is to import the data in the system Identification app. The user is required to give the input and output of the system (in the time domain) alongside with the sample time. An optional step is to give the data a name, in the data information window.

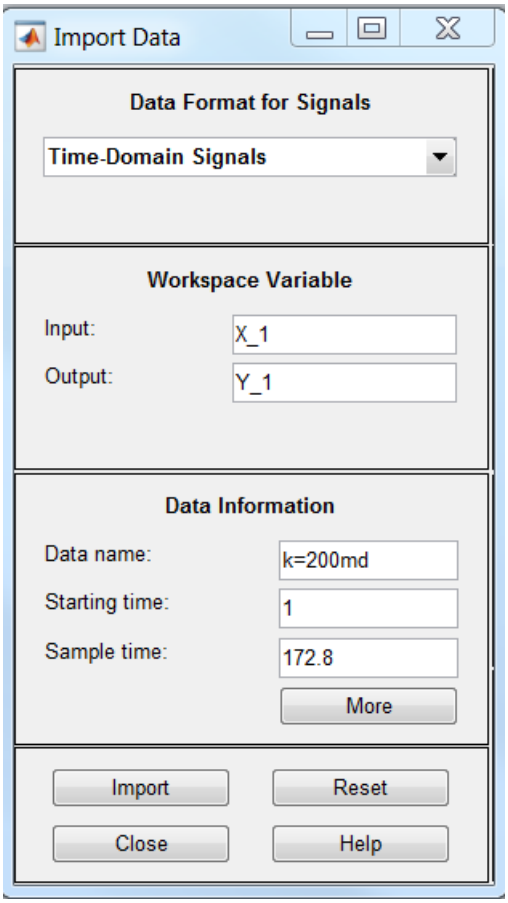

Figure B.1: Importing signals into Matlab System Identification toolbox.

After importing the data, the transfer function can be estimated in the SystemIdentification app. This is done with making the data active. The transfer function is based on a discrete time signal and therefore the radio button 'Discrete-time signal' needs to be selected. The number of poles and zeros are required for estimation of the transfer function.

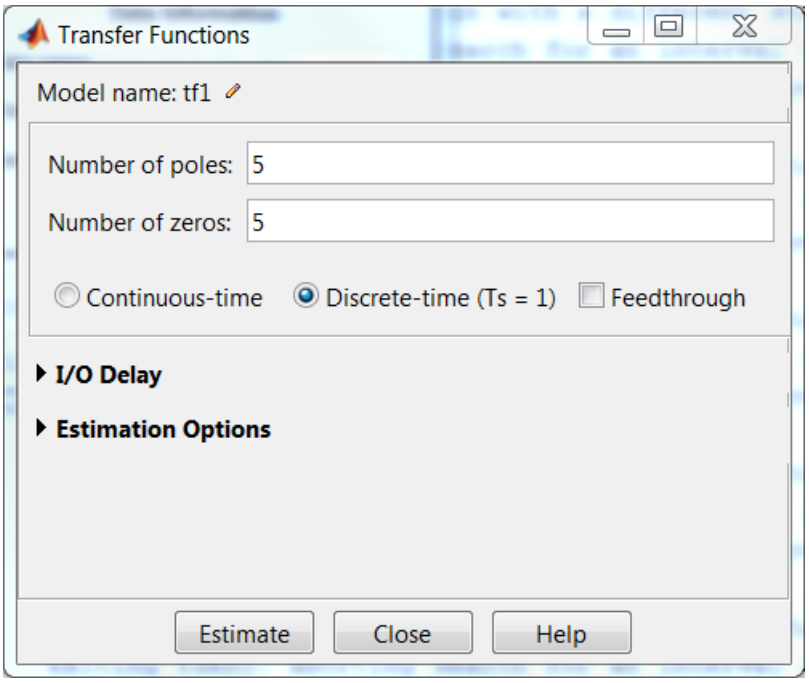

Figure B.2: Estimating transfer function with the SI toolbox.

Coming back to the System Identification app, we now can export the transfer function and use a Matlab script to plot the data. The other method is two use a scripted method, which is explained by the Matlab code in the lines below. Working with the scripted/command line method saves time.

```
% System Identification to estimate transfer function based on
pressure and net flow rate measurements for segment i

% 1. Import data as an data object with iddata, which can be used to
estimate the transfer
% fuction with inputs:
%
% p_sf_i = pressure at sand face (compared to steady state)for
segment i
% q_net_i = net inflow rate for segment i
% t_step = time in secondes between measurements
% output:
% PTA_i = data object with PTA data for segment i in the time domain
PTA_i = iddata(p_sf_i, q_net_i, t_step);

% 2. estimate transfer function R12_mes_i in frequency domain with
tfest
% inputs:
% PTA_i = data object with PTA data for segment i in time domain
% Np = number of poles
% Nz = number of zeros
% PTA_i.Ts = t_step in secondes
% 'feedtrough' = true;
% output:
% R12_mes_i = estimated transfer function based on measurements in
the frequency domain
R12_mes_i = tfest(PTA_i, Np, Nz, 'Ts', PTA_i.Ts, 'feedthrough',
true)
```

Appendix C. Derivation of the radial diffusivity equation in the Laplace domain for SI [2]

The radial diffusivity equation for a homogenous porous medium for single phase liquid radial flow in the radial direction is given by,

$$\frac{1}{r}\frac{\partial}{\partial r}r\frac{\partial p(r,t)}{\partial r}=\frac{1}{\eta}\frac{\partial p(r,t)}{\partial t}, \tag{C.1}$$

where *r* is the radial coordinate and η is called the hydraulic diffusivity,

$$\eta=\frac{k}{\mu\phi c_t}, \tag{C.2}$$

where *k* is the permeability, μ is the viscosity, ϕ is the porosity and c_t is the total rock compressibility. An assumption is made that the compressibility is constant, which implies that η is also constant, leaving a linearized equation, which is similar to the heat conduction in a radial symmetry described in [2]. The initial conditions are that the pressure represents the difference with respect to steady-state conditions and the radial,

$$p(r,0)=0, \qquad r_w<r\leq r_e. \tag{C.3}$$

The first step is to convert equation C.1. to the Laplace domain:

$$r\frac{\partial}{\partial r}r\frac{\partial P(r,s)}{\partial r}=\frac{s}{\eta}r^2P(r,s), \tag{C.4}$$

where s is the Laplace parameter. The solution for the pressure in the radial coordinate is obtained by solving the ordinary-differential equation C.3,

$$P(r,s)=M_1I_0\left(\sqrt{\frac{s}{\eta}}r\right)+M_2K_0\left(\sqrt{\frac{s}{\eta}}r\right), \tag{C.5}$$

where M_1 and M_2 are two arbitrary coefficients and I_0 and K_0 are zero order modified Bessel functions of respectively the first and second kind. To find the magnitudes M_1 and M_2, we transform Darcy's law,

$$q(r,t)=-\frac{2\pi rkh}{\mu}\frac{\partial p(r,t)}{\partial r}, \tag{C.6}$$

where *h* is defined as the reservoir height, to the Laplace domain,

$$Q(r,s)=-\frac{2\pi kh}{\mu}\left[M_1r\sqrt{\frac{s}{\eta}}I_1\left(\sqrt{\frac{s}{\eta}}r\right)-M_2r\sqrt{\frac{s}{\eta}}K_1\left(\sqrt{\frac{s}{\eta}}r\right)\right], \tag{C.7}$$

where I_1 and K_1 are first order modified Bessel functions. Note that the reservoir height *h* in the case of SI for DPS will be the length of a well segment. Two boundary conditions are required to find M_1 and M_2 of equations C.5 and C.7. We assume that the flow rate at the outer boundary $Q_{r_e}=Q(r_e,s)$ and the pressure at the sand face $P_{sf}=P(r_w,s)$ are known. M_1 and M_2 for these conditions are determined to be,

$$M_1 = \frac{K_1\left(r_e\sqrt{\frac{s}{\eta}}\right)P_{sf} - \frac{1}{T}\,K_0\left(r_w\sqrt{\frac{s}{\eta}}\right)Q_{r_e}}{I_1\left(r_e\sqrt{\frac{s}{\eta}}\right)K_0\left(r_w\sqrt{\frac{s}{\eta}}\right) + \,I_0\left(r_w\sqrt{\frac{s}{\eta}}\right)K_1\left(r_e\sqrt{\frac{s}{\eta}}\right)}, \tag{C.8}$$

and,

$$M_2 = \frac{I_1\left(r_e\sqrt{\frac{s}{\eta}}\right)P_{sf} - \frac{1}{T}\,I_0\left(r_w\sqrt{\frac{s}{\eta}}\right)Q_{r_e}}{I_1\left(r_e\sqrt{\frac{s}{\eta}}\right)K_0\left(r_w\sqrt{\frac{s}{\eta}}\right) + \,I_0\left(r_w\sqrt{\frac{s}{\eta}}\right)K_1\left(r_e\sqrt{\frac{s}{\eta}}\right)}, \tag{C.9}$$

where *T* is,

$$T = -\frac{2\pi kh}{\mu}\,r_e\sqrt{\frac{s}{\eta}}. \tag{C.10}$$

With the coefficients M_1 and M_2 defined in equations C.8 and C.9, we can solve equations C.5 and C.7 for the flow rate at the sand face $Q_{sf} = Q(r_w, s)$, and the pressure at the boundary of the reservoir $P_{r_e} = P(r_e, s)$. This leads to an relationship between Q_{sf}, Q_{r_e}, P_{sf} and P_{r_e} which is the dynamical behaviour of the reservoir. The connection between the variables can be expressed by the casual structure as seen in Figure C.1 and by the following set of equations,

$$\begin{bmatrix} Q_{sf} \\ P_e \end{bmatrix} = \mathbb{R}\begin{bmatrix} Q_e \\ P_{sf} \end{bmatrix} = \begin{bmatrix} R_{11} & R_{12} \\ R_{21} & R_{22} \end{bmatrix}\begin{bmatrix} Q_e \\ P_{sf} \end{bmatrix}, \tag{C.11}$$

where $\mathbb{R}$ is a 2-by-2 matrix consisting of transfer function which are,

$$R_{11}(s) = \frac{r_w}{r_e}\frac{I_1\left(r_w\sqrt{\frac{s}{\eta}}\right)K_0\left(r_w\frac{\sqrt{s}}{\eta}\right) + K_1\left(r_w\sqrt{\frac{s}{\eta}}\right)I_0\left(r_w\frac{\sqrt{s}}{\eta}\right)}{I_1\left(r_e\sqrt{\frac{s}{\eta}}\right)K_0\left(r_w\frac{\sqrt{s}}{\eta}\right) + I_0\left(r_w\sqrt{\frac{s}{\eta}}\right)K_1\left(r_e\frac{\sqrt{s}}{\eta}\right)}, \tag{C.12}$$

$$R_{12}(s) = T\frac{r_w}{r_e}\frac{I_1\left(r_w\sqrt{\frac{s}{\eta}}\right)K_1\left(r_e\frac{\sqrt{s}}{\eta}\right) - K_1\left(r_w\sqrt{\frac{s}{\eta}}\right)I_1\left(r_e\frac{\sqrt{s}}{\eta}\right)}{I_1\left(r_e\sqrt{\frac{s}{\eta}}\right)K_0\left(r_w\frac{\sqrt{s}}{\eta}\right) + I_0\left(r_w\sqrt{\frac{s}{\eta}}\right)K_1\left(r_e\frac{\sqrt{s}}{\eta}\right)}, \tag{C.13}$$

$$R_{21}(s) = \frac{I_0\left(r_e\sqrt{\frac{s}{\eta}}\right)K_0\left(r_w\frac{\sqrt{s}}{\eta}\right) - K_0\left(r_e\sqrt{\frac{s}{\eta}}\right)I_0\left(r_w\frac{\sqrt{s}}{\eta}\right)}{I_1\left(r_e\sqrt{\frac{s}{\eta}}\right)K_0\left(r_w\frac{\sqrt{s}}{\eta}\right) + I_0\left(r_w\sqrt{\frac{s}{\eta}}\right)K_1\left(r_e\frac{\sqrt{s}}{\eta}\right)}, \tag{C.14}$$

$$R_{22}(s) = \frac{I_0\left(r_e\sqrt{\frac{s}{\eta}}\right)K_1\left(r_e\frac{\sqrt{s}}{\eta}\right) + K_0\left(r_e\sqrt{\frac{s}{\eta}}\right)I_1\left(r_e\frac{\sqrt{s}}{\eta}\right)}{I_1\left(r_e\sqrt{\frac{s}{\eta}}\right)K_0\left(r_w\frac{\sqrt{s}}{\eta}\right) + I_0\left(r_w\sqrt{\frac{s}{\eta}}\right)K_1\left(r_e\frac{\sqrt{s}}{\eta}\right)}. \quad \text{(C.15)}$$

For pressure transient analysis (PTA), we are interested in the change of pressure at the sand face during the transient regime, i.e., when the flow rate at the exterior boundary is zero. This implies that transfer functions R_{12} provides a direct relationship between the change in pressure and flow rate at the sand face, see Figure C.1 and equation C.13.

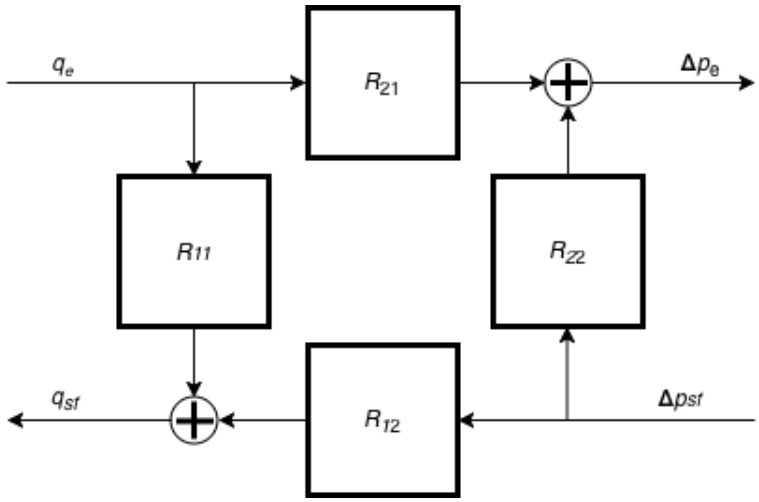

Figure C.1: Casual representation of the reservoir model, showing the relationship between inputs and outputs.